Species-Dependent Energy Transfer of Surfactant-Dispersed Semiconducting Single-Walled Carbon Nanotubes

ARTICLE *in* THE JOURNAL OF PHYSICAL CHEMISTRY C · NOVEMBER 2009

Impact Factor: 4.77 · DOI: 10.1021/jp9076883

8 AUTHORS, INCLUDING:

Jun Ye
Institute Of High Performance Computing
28 PUBLICATIONS **377** CITATIONS
SEE PROFILE

Yang Zhao
China Institute of Water Resources and Hy…
150 PUBLICATIONS **1,638** CITATIONS
SEE PROFILE

Lay Poh Tan
Nanyang Technological University
91 PUBLICATIONS **1,427** CITATIONS
SEE PROFILE

Yuan Chen
University of Sydney
127 PUBLICATIONS **3,763** CITATIONS
SEE PROFILE

Species-Dependent Energy Transfer of Surfactant-Dispersed Semiconducting Single-Walled Carbon Nanotubes

Fuming Chen,[†] Jun Ye,[†] Ming Yong Teo,[†] Yang Zhao,[†] Lay Poh Tan,[†] Yuan Chen,[‡] Mary B. Chan-Park,[‡] and Lain-Jong Li*[,†]

School of Materials Science and Engineering, Nanyang Technological University, 50 Nanyang Ave. Singapore, 639798, School of Chemical and Biomedical Engineering, Nanyang Technological University, Singapore, 637459

Received: August 10, 2009; Revised Manuscript Received: October 1, 2009

Single-walled carbon nanotubes (SWNTs) are stabilized with sodium dodecyl sulfate (SDS) micelles in aqueous solution. Aggregation among semiconducting SWNTs can be identified by exciton energy transfer (EET) features in photoluminescence excitation (PLE) mapping. Addition of *o*-dichlorobenzene (ODCB) not only changes the micelle structure but also induces the aggregation among SWNT species, leading to drastic changes in the EET features of the ensemble. Force-field and molecular dynamic simulation confirm that SWNT bundles are energetically favorable at room temperature. Observed EET features in PLE mappings are found to be SWNT species-dependent. Moreover, the rapid bundling process induced by ODCB allows us to obtain SWNT bundles which are potentially useful for optical and optoelectronic applications.

Introduction

Photoluminescence excitation (PLE) mapping is one of the important methodologies to identify the chirality of individually dispersed semiconducting SWNTs. Tremendous efforts have been spent to study photoluminescence behavior of dispersed individual SWNTs.[1−29] Photoluminescence spectra are sensitive to environmental factors such as solvents,[12] wrapping surfactants, or polymers,[13−20] temperature,[21−23] magnetic fields,[23−25] electric fields,[26] mechanical strain,[27] doping states,[28] and tube aggregation states.[29] Recently, a few studies have reported the photoluminescence behavior of SWNT bundles.[30−34] The energy transfer features observed in the PLE mapping were ascribed to the fact that the excitonic energy is transferred from the SWNTs with larger energy gaps (we called them donor tubes here because they tend to donate excitonic energy) to the neighboring tubes with smaller energy gaps (thus named acceptor tubes) within the same bundle. This process leads to the enhanced photoluminescence from acceptor tubes.[33,34] A similar energy transfer process has also been observed in a single pair of individual air-suspended SWNTs which were formed accidentally during synthesized process.[30−32] The efficiency of energy transfer from large-gap SWNTs is very high, sometimes comparable or even higher than nonradiative recombination in itself.[33,34] Hence, the semiconducting SWNT bundles may be used for optoelectronic applications, for example, converting high energy photons absorbed by donor tubes to desired low energy photons emitted from acceptor tubes (down-conversion of photons). Therefore, the aggregation of semiconducting tubes and the energy transfer processes in SWNT bundles merit in-depth investigations.

Wang et al. has reported that the structure of SDS micelles can be altered by adding organic solvents such as chloroform or *o*-dichlorobenzene (ODCB) into the SDS-stabilized aqueous SWNT suspensions.[35] The optical band gaps and peak intensity of the tubes existed in the micelles shall be changed, which is known as the solvatochromic effect. Our PLE mappings confirm that the addition of ODCB quenches the PL from SDS-dispersed SWNTs. In addition, evaporation of residual ODCB from the SWNT-micelle system significantly changes the energy transfer channels among semiconducting SWNTs. This suggests that ODCB-induced micelle-reorganization promotes formation of bundles, and these newly formed or reorganized bundles are still small in size such that their luminescent behavior is not suppressed by the metallic SWNT species. Force-field and molecular dynamics (MD) studies confirm that these bundles are stable at room temperature. In addition, the energy transfer route exhibits obvious species dependence. For example, (6,4) prefers to transfer energy to (10,2) rather than (6,5). The formation of species-dependent energy transfer routes is likely not due to the preferential formation of species-dependent bundles.

Experimental Section

Sample Preparation and Measurements. Purified CoMoCat76 SWNTs were purchased from Southwest NanoTechnologies (USA) and used as received without further purification. SWNT powders (2 mg) were dispersed in a 1 wt % sodium dodecyl sulfate (SDS) aqueous solution (20 mL). The solution was then homogenized in a sonic bath for 30 min followed by probe sonication for 30 min at a power level of 120 W. It was then promptly followed by centrifugation at 140 000 $\times g$ for 1.5 h. A 4-mL portion of the obtained supernatant was then mixed with 2 mL of ODCB. The mixture was shaken vigorously for 5 min with a vortex stirrer to form a white emulsion. After shaking, the white emulsion began to be separated into aqueous and organic phases. The characterization of aqueous SWNTs suspensions was done after layover for 12 h to reach steady state. For the ODCB evaporation experiments, the previously obtained aqueous SWNT suspensions were kept open to the ambient and left in a fume hood for desired period of time (24 to 72 h). Ultraviolet visible near-infrared (UV−vis−NIR) absorption spectra were measured in a Perkin−Elmer Lambda

* To whom correspondence should be addressed. E-mail: ljli@ntu.edu.sg.
[†] School of Materials Science and Engineering.
[‡] School of Chemical and Biomedical Engineering.

10.1021/jp9076883 CCC: $40.75
Published on Web 10/19/2009

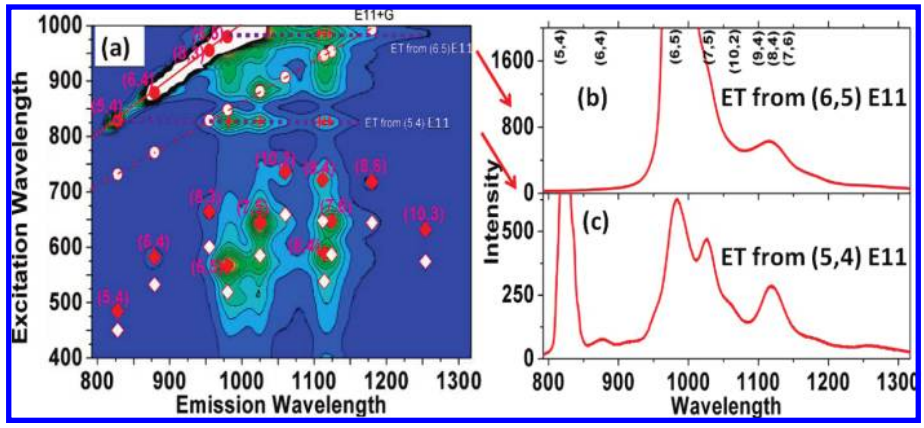

Figure 1. (a) PLE map for as-prepared SDS-dispersed SWNT suspension. Eleven major species (5,4), (6,4), (6,5), (8,3), (7,5), (10,2), (7,6), (9,4), (8,4), (8,6), and (10,3) are identified. Excitation satellites from bundled tubes and from phonon-assisted photoexcitation are also indicated. The E_{11} + G photoexcitations are denoted by open circles ○ while the E_{22} + G photoexcitations are indicated as open diamonds ◇. (b,c) The PL spectra of the suspension excited at the E_{11} absorption energies of (b) (6,5) and (c) (5,4), respectively.

900 spectrometer. Fluorescence characterization was performed on a Jobin−Yvon Horiba Fluorolog-3 spectrofluorometer with an electrically cooled InGaAs detector.

Simulation Methods. The Forcite module integrated in the Materials Studio package is used to search for minimal-energy configurations of the SWNT bundles, and the consistent-valence force-field (CVFF)[36] is chosen for a better description of the van der Waals interactions between conjugated carbon atoms. To examine whether the bundling process is species-dependent, without loss of generality, it is assumed that each CNT bundle was composed of 7 carbon nanotubes ~100 nm in length (1 acceptor tube in the middle surrounded by 6 donor tubes). Although this length is about 10× smaller than what have been observed in our AFM experiment, we believe the model should capture to some extent the qualitative behavior in our SWNT sample. The geometry optimizations are performed for the bundles by requiring: energy difference $<2.0 \times 10^{-5}$kcal/mol, force difference <0.001 kcal/mol/Å and displacement difference $<1.0 \times 10^{-5}$ Å. For the calculation of electrostatic and van der Waals (vdW) energies, the cutoff distance of 18.5 Å was applied.

To evaluate the strength of interaction between the donor and acceptor tubes, calculations have also been performed for individual tubes with the aforementioned convergence criteria. The intertube binding energy is then defined as the differences between the energy of the bundled structure and that of isolated SWNTs, $E_{tot} = E_{tot}(\text{bundle}) - E_{tot}(\text{acceptor}) - n \times E_{tot}(\text{donor})$, where n is the number of donor tubes in the bundle.

In performing molecular dynamics simulation, the canonical ensemble (NVT) is chosen for investigating the effect of temperature on the structure of the bundle. The total running time for each bundle is set at 100 ps with a time step of 1 fs. The Berendsen thermostat is used with decay time of 0.1 ps. The force field used was also CVFF.

Results and Discussions

Figure 1(a) shows the PLE map from the as-prepared SDS-dispersed SWNT solution. We monitor the NIR emissions from various semiconducting SWNT species by excitation with a wide-range of wavelengths (400−1000 nm), covering from UV to NIR. On the basis of the emission wavelength from first van Hove band gap (E_{11}) and the resonance excitation wavelength of their second van Hove band gaps (E_{22}), eleven major SWNT chiral species (5,4), (6,4), (6,5), (8,3), (7,5), (10,2), (7,6), (9,4), (8,4), (8,6), and (10,3) are identified in Figure 1(a). Excitation satellites from bundled tubes[30−34] and from phonon-assisted emissions[37−39] are also indentified. Following Lebedkin's work,[37] we attribute most of the satellite peaks to phonon-coupled photoexcitations, as indicated in Figure 1(a). In addition, the excitation at 828 and 980 nm results in the emission from many other SWNT species. On the basis of Tan's work,[33,34] the 828 nm excitation directly generates the excitons through the E_{11} gap of (5, 4) tubes in bundles and the excitons subsequently transfer to adjacent species, resulting in the emissions of tubes with smaller gaps such as (6,5), (7,5) and larger diameter tubes such as (9,4), (7,6), or (8,4). Similarly, the excitation 980 nm causes the energy transfer from (6,5) to (7,5) and other species. These EET features were indicated by the dotted lines in the Figure 1(a) and PL spectra excited at the corresponding wavelengths were shown in Figure 1, parts (b) and (c).

ODCB was rigorously mixed with the as-prepared SDS-dispersed SWNT solution and then the aqueous phase was extracted after layover for 12 h, where the SDS micelles in the aqueous phase were incorporated with some ODCB molecules.[35] Figure 2(a) shows the PLE mapping of the aqueous suspension after incorporating ODCB. The E_{11} fluorescence peaks of these species excited directly from their E_{22} transitions were significantly quenched, almost undetectable on the PLE map. Figure 3 shows that the absorption peaks for the SWNT species are largely suppressed and red-shifted by 3−11 nm after ODCB addition. The absorption and PL spectral changes imply that the ODCB molecules are in close proximity of the nanotubes and the hydrophobic region of the micelles surrounding SWNTs swells with the organic solvent when mixed,[35] resulting in increased exposure to quenching mechanisms from the aqueous phase.[40] It is noted that the EET features observed in Figure 1(a) are still present in Figure 2(a). Because the emissions from individual semiconducting SWNTs (excited at their E_{22} gaps) are largely quenched by water, such energy transfer phenomena could only occur between adjacent tubes in the bundles, where the excitons formed in the SWNTs embedded in bundles are not easily accessed by water molecules.

In addition to the previously observed PL features (Figure 1) caused by the EET from E_{11} band gap excitation of (6,5) and (5,4), Figure 2(a) shows several new PL peaks with the excitation at ~456 nm (indicated with the horizontal dash line). These peaks are unlikely from E_{33} resonance excitation for each identified tube owing to the mismatch between observed and expected [indicated as solid triangle in Figure 2(b)] PLE peak

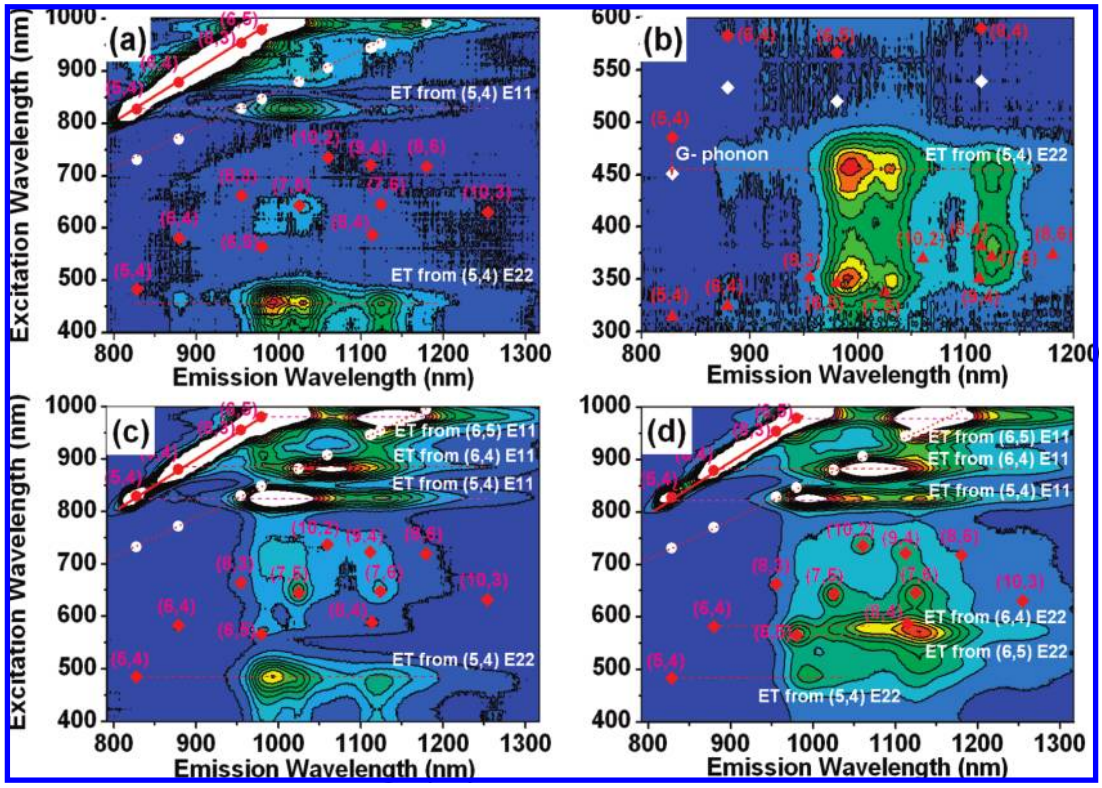

Figure 2. (a) PLE and (b) zoomed in PLE for aqueous SWNT suspensions mixed with *o*-dichlorobenzene after waiting for 12 h to reach steady state, where solid triangle (▲) represents the expected PL from E_{33} excitations of each SWNTs. (c,d) PLE maps after evaporation in ambient for 24 h (c) and (d) 72 h.

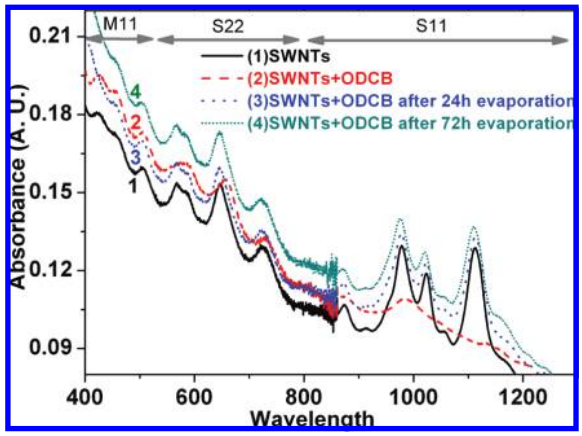

Figure 3. Absorbance spectra of as-prepared CNT suspensions (solid 1), aqueous CNT suspensions mixed with ODCB after waiting for 12 h to reach steady state (dash 2), after ODCB evaporation for 24 h (dot 3) and those after evaporation for 72 h (short dot 4).

positions.[6] Figure 2(b) shows that the emission wavelengths of the peaks at around 992 and 1029 nm correspond to the E_{11} emission wavelengths of the species (6,5) and (7,5), respectively,[6,13−15] and the PL emission at 1125 nm may be attributed to the (8,4), (7,6), and (9,4) species. All of these peaks are well aligned at the excitation wavelength 456 nm; therefore, these features are likely caused by the EET process from a large-gap SWNT. It is interesting to point out that the resonance excitation energy 2.72 eV (wavelength 456 nm) matches to the sum of the E_{22} gap energy of (5,4) (2.52 eV) and the G-band phonon energy (0.20 eV). This suggests that these EET features were caused by the phonon-assisted photoexcitations of (5,4) species in the bundles. The energy transfer from (5,4) by its E_{22}+G excitation is more efficient than that from other species by their E_{11} excitation, as can be seen from the relatively stronger NIR emission from acceptor tubes. It could be due to that the E_{11} excitons are more prone to water quenching, compared with E_{22} excitons in (5,4) SWNTs. In addition, due to the severe quenching of the PL peaks caused by solvatochromic effect, the observation of energy transfer from E_{22} excitons of (5,4) to other tube species suggests that the presence of small bundles is indeed favored in the ODCB environment.

Upon evaporation of ODCB from the same suspension for 24 h and 72 h, the surfactant structure returns to the state which is better protected against water-quenching, thereby improving the fluorescence intensity, as shown in Figure 2, parts (c) and (d), respectively. Such recovery of PL intensities is in good agreement with previous observations.[35] It is noted that Figure 2, parts (a), (c), and (d) are plotted with different false color map scales (z-scale) in order to clearly demonstrate the PL features in each map. We have also plotted in Figure S1 of the Supporting Information three graphs using the same false color scale, which allows a comparison of absolute PL intensities.

The emissions caused by energy transfer from E_{11} and E_{22} excitons of (5,4) species were still present upon ODCB evaporation, and those caused by the E_{11} excitation become even stronger in the intensity than those from the E_{22} excitation. This corroborates our previous suggestion that E_{11} excitons are more sensitive to the change of the environments than the E_{22} excitons. In addition, new series of energy transfer peaks emerged after the evaporation of ODCB, as shown in Figure 2, parts (c) and (d). For example, the presence of the EET peaks excited at around 880 nm, corresponding to the E_{11} energy of (6,4) nanotubes, suggests that the energy transfer path from (6, 4) to (10, 2) is activated. As such, incorporation of ODCB into the micelle environment could therefore activate SWNT aggregation (or the formation of small bundles). Similarly, the PL emissions from the donor−acceptor pairs associated with (5,4), (6,5), or

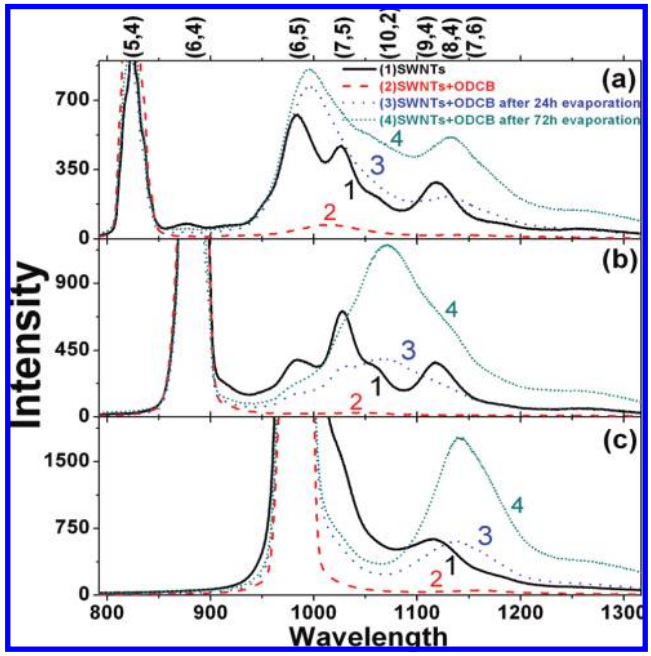

Figure 4. The effect of ODCB addition and evaporation on the arbitrary intensity of EET features through the excitation of E_{11} gap of (a) (5,4), (b) (6,4), and (c) (6,5), respectively.

(6,4) donor tube were much enhanced after 24 h ODCB evaporation. Figure 4 shows the effect of ODCB addition and evaporation on the arbitrary intensity of EET features through the E_{11} excitations with (5,4), (6,4), and (6,5) donor tubes. The emergence of new energy transfer channels shown in the PLE maps strongly supports the formation or reorganization of SWNT bundles.

We would like to comment on the relation between micelle structures and the optical features of SWNTs. Figure 3 displays the absorption spectra for the 4 suspensions discussed in Figures 1 and 2. The absorption peaks of the suspension after mixing with ODCB (red dashed line) are notably broadened and red-shifted. Since the better-resolved peaks reappear after 24 h evaporation of ODCB, this implies that the nanotube species have been optically dark but still present in the aqueous phase. Also, a small additional blueshift is observed for the solution after 72 h evaporation, compared to the initial curve (black solid line) due to the micelle reorganization.[35] This points to that the absorption peaks are strongly affected by the imperfection of micelle or SDS arrangement on SWNTs. It is noted that the peak width in absorption features is an indicator of the bundling state; the peak width increases if tubes are bundled.[33] Unexpectedly, the spectral peaks do not exhibit significantly broader widths after the evaporation of ODCB. It is speculated that the micelle reconstruction effect on absorption peaks is stronger than the effect from the formation of small bundles. Alternatively, it is also possible that only a small portion of SWNT aggregates into bundles, detectable in PL rather than absorption spectra. It is noteworthy that if we perform short sonication to the solution (after 72 h evaporation), the PLE map in the initial solution can be recovered (Figure 1). This observation points to that the bundled tubes are redissociated by ultrasonication, which corroborates our previous argument that bundles are formed with the ODCB treatment.

Although metallic SWNTs are not the focus of discussion due to the absence of PL, it is noteworthy that the E_{11} absorption peaks of the metallic tubes are not affected by the inclusion of ODCB, as shown in Figure 3. This is in clear contrast to semiconducting tubes. The ODCB-insensitive absorption features of metallic species could be related to that the E_{11} singularity points in their electronic structure are far from the Fermi energy. Therefore, more carriers need to be removed (or added) in order to alter their absorption-spectral features. Exact mechanisms behind this observation still await further investigations.

TABLE 1: Donor and Associated Acceptor Tubes Revealed from PLE Mappings[a]

donor tube	associated acceptor tube
(5,4)	(6,5), (7,5), (6,4), (10,2), (9,4),(8,4)
(6,4)	(10,2), (7,5), (6,5),(8,4),(7,6),(9,4)
(6,5)	(8,4), (7,5), (9,4),(10,2),(7,6)

[a] The acceptor tube species underlined stand for the tubes with stronger PL intensity caused by energy transfer from the corresponding donor tube.

On the basis of the energy transfer behavior previously discussed, several sets of donor and associated acceptor tubes were identified and summarized in Table 1. To find out whether the bundling process is species-dependent, force field calculations and molecular dynamics simulation are performed. It is known that a good dispersion of nanotubes achieved through sonication may consist of small bundles, i.e., 2, 3, or 4 tubes in a bundle. However, these small bundles are prone to PL quench due to large exposed areas of acceptor tubes to the surrounding water molecules. Thus, the tightly wrapped bundle structure as shown in Figure 5, where one tube is shielded by 6 tubes, is adopted to simulate the experimental observations. We assume that each SWNT's bundle is composed of seven carbon nanotubes ~100 nm in length (1 center acceptor tube surrounded by 6 donor tubes). Figure 5(a) shows the optimized structure for a (10,2) tube bundled with six (6,4) tubes, and the structure after a 100 ps MD run is shown in Figure 5(b) for comparison. The intertube van der Waals energies for various tube combinations are listed in Table S1(a) of the Supporting Information. Energetically, the bundle formation is preferred as it reduces the total energy of the bundle. The lowering of the energy for each atom is about twice k_BT where $T = 300$ K. The mean square displacements (MSD) of the donor tubes for these combinations are shown in Figure S2 of the Supporting Information. The donor tubes are shown to have relatively large xx', yy', and zz' Cartesian anisotropic components compared to the others (i.e., xy', xz', and yz'), suggesting stable bundles are formed between donor and acceptor tubes since the motions of the donor tubes are dominated by those slipping along axial direction of the acceptor tubes. After thermal equilibration, no obvious structural changes were observed from the trajectories of the bundles, as shown in Figure 5. Both static and dynamic results lend support to that SWNT bundles are stable at room temperature. From the data in Table S1(a) of the Supporting Information, it is concluded that the binding energies vary little, and the bundle formation is species-independent. We have also calculated the binding energies for the tube bundles consisting only 2 to 4 tubes, as shown in Table S1(b)−(d) of the Supporting Information. In general, the bundles consisting 7 tubes are energetically more preferable compared with smaller size bundles according to the results in Table S2 of the Supporting Information. Also, the binding energy for small size bundle formation is species-independent. Therefore, the observed species-dependent energy transfer process is more likely controlled by the preferential carrier pathways associated with the electronic band alignment of donor−acceptor tubes. The separation of these bundles is required to test on their PL efficiency for further verifying this hypothesis.

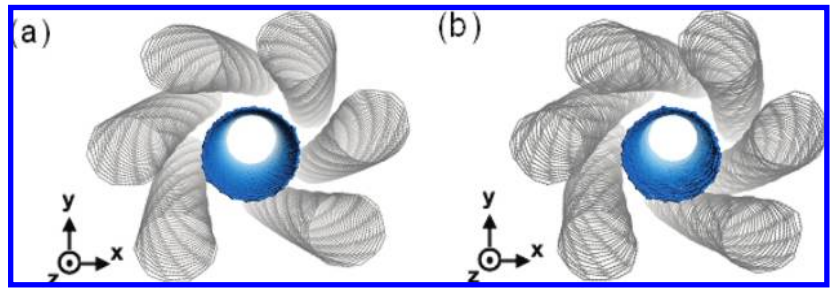

Figure 5. The structure of the bundle Shell:6 × (6,4) + Core: 1 × (10,2) (a) after geometry optimization with force-field method, an (b) after molecular dynamic runs. The axial direction of the core tube is parallel the *z*-axis, as shown.

Conclusions

In summary, we present a thorough photoluminescence study of aqueous SWNT suspensions mixed with OBCD. The introduction of ODCB into the aqueous SWNT suspensions affects photoluminescence in two ways. On one hand, solvatochromic shifts in the absorbance and fluorescence spectra appear when surfactant-stabilized aqueous SWNTS suspensions are mixed with ODCB. On the other hand, addition of ODCB to the micelle environment helps in the rapid formation of tube bundles, resulting in more intense energy transfer peaks among these tubes. The force-field calculation and molecular dynamics simulation suggest that bundles are energetically stable at room temperature. However, the bundling process lacks species-selectivity. The observed chiral dependence of intertube energy transfer is likely not due to the preferential formation of species-dependent bundles. We also observe that the (5,4) E_{11} excitons seem to be more sensitive to the environmental changes compared with its E_{22} excitons. The rapid bundling process induced by organic solvent allows us to obtain optically active bundles with promising optical and optoelectronic applications such as down-conversion of photons, photodetectors, and phototransistors.

Acknowledgment. This research was supported by National Research Foundation Singapore (NRF-CRP 2−2007−02).

Supporting Information Available: Photoluminescence excitation maps and calculation results with force-field methods. This information is available free of charge via the Internet at http://pubs.acs.org.

References and Notes

(1) O'Connell, M. J.; Bachilo, S. H.; Huffman, C. B.; Moore, V. C.; Strano, M. S.; Haroz, E. H.; Rialon, K. L.; Boul, P. J.; Noon, W. H.; Kittrell, C.; Ma, J.; Hauge, R. H.; Weisman, R. B.; Smalley, R. E. *Science* **2002**, *297*, 593.

(2) Bachilo, S. M.; Strano, M. S.; Kittrell, C.; Hauge, R. H.; Smalley, R. E.; Weisman, R. B. *Science* **2002**, *298*, 2361.

(3) Dresselhaus, M. S.; Dresselhaus, G.; Saito, R.; Jorio, A. *Annu. Rev. Phys. Chem.* **2007**, *58*, 719.

(4) Torrens, O. N.; Milkie, D. E.; Zheng, M.; Kikkawa, J. M. *Nano Lett.* **2006**, *6*, 2864.

(5) Oyama, Y.; Saito, R.; Sato, K.; Jiang, J.; Samsonidze, G. G.; Gruneis, A.; Miyauchi, Y.; Maruyama, S.; Jorio, A.; Dresselhaus, G.; Dresselhaus, M. S. *Carbon* **2006**, *44*, 873.

(6) Chen, F.; Zhang, W.; Jia, M.; Wei, L; Fan, X.-F.; Kuo, J.-L.; Chen, Y.; Chan-Park, M.-B.; Xia, A.; Li, L.-J. *J. Phys. Chem. C* **2009**, *113*, 14946.

(7) Weisman, R. B.; Bachilo, S. M. *Nano Lett.* **2003**, *3*, 1235.

(8) Cherukuri, P.; Bachilo, S. M.; Litovsky, S. H.; Weisman, R. B. *J. Am. Chem. Soc.* **2004**, *126*, 15638.

(9) Umeyama, T.; Kadota, N.; Tezuka, N.; Matano, Y.; Imahori, H. *Chem. Phys. Lett.* **2007**, *444*, 263.

(10) Zhang, L.; Tu, X.; Welsher, K.; Wang, X.; Zheng, M.; Dai, H. *J. Am. Chem. Soc.* **2009**, *131*, 2454.

(11) Sun, X.; Zaric, S.; Daranciang, D.; Welsher, K.; Lu, Y.; Li, X.; Dai, H. *J. Am. Chem. Soc.* **2008**, *130*, 6551.

(12) Hwang, J.-Y.; Nish, A.; Doig, J.; Douven, S.; Chen, C.-W.; Chen, L.-C.; Nicholas, R. J. *J. Am. Chem. Soc.* **2008**, *130*, 3543.

(13) Nish, A.; Hwang, J.-Y.; Doig, J.; Nicholas, R. J. *Nat. Nanotechnol.* **2007**, *2*, 640.

(14) Chen, F.; Wang, B.; Chen, Y.; Li, L. J. *Nano lett.* **2007**, *7*, 3013.

(15) Izard, N.; Kazaoui, S.; Hata, K.; Okazaki, T.; Saito, T.; Iijima, S.; Minami, M. *Appl. Phys. Lett.* **2008**, *92*, 243112.

(16) Cheng, F.; Imin, P.; Maunders, C.; Botton, G.; Adronov, A. *Macromolecules* **2008**, *41*, 2304.

(17) Hasan, T.; Scardaci, V.; Tan, P. H.; Rozhin, A. G.; Milne, W. I.; Ferrari, A. C. *Physica E* **2008**, *40*, 2414.

(18) Hasan, T.; Tan, P. H.; Bonaccorso, F.; Rozhin, A. G.; Scardaci, V.; Milne, W. I.; Ferrari, A. C. *J. Phys. Chem. C* **2008**, *112*, 20227.

(19) Star, A.; Stoddart, J. F. *Macromolecules* **2002**, *35*, 7516.

(20) Ju, S.-Y.; Kopcha, W. P.; Papadimitrakopoulos, F. *Science* **2009**, *323*, 1319.

(21) Lefebvre, J.; Finnie, P.; Homma, Y. *Phys. Rev. B* **2004**, *70*, 045419.

(22) Li, L.-J.; Nicholas, R. J.; Chen, C.-Y.; Darton, R. C.; Baker, S. C. *Nanotechnology* **2005**, *16*, S202.

(23) Nicholas, R. J.; Mortimer, I. B.; Li, L.-J.; Nish, A.; Portugall, O.; Rikken, G. L. J. A *Int. J. Mod. Phys. B* **2007**, *21*, 1180.

(24) Shaver, J; Kono, J.; Portugall, O.; Krstic, V.; Rikken, X. G. L. J. A.; Miyauchi, Y.; Maruyama, S.; Perebeinos, V *Nano Lett.* **2007**, *7*, 1851.

(25) Zaric, S.; Ostojic, G. N.; Kono, J.; Shaver, J.; Moore, V. C.; Hauge, R. H.; Smalley, R. E.; Wei, X. *Nano Lett.* **2004**, *4*, 2219.

(26) Naumov, A. V.; Bachilo, S. M.; Tsyboulski, D. A.; Weisman, R. B. *Nano Lett.* **2008**, *8*, 1527.

(27) Kaniber, S. M.; Song, L.; Kotthaus, J. P.; Holleitner, A. W. *Appl. Phys. Lett.* **2009**, *94*, 261106.

(28) Sáfar, G. A. M.; Ribeiro, H. B.; Malard, L. M.; Plentz, F. O.; Fantini, C.; Santos, A. P.; Freitas-Silva, G.; Idemori, Y. M. *Chem. Phys. Lett.* **2008**, *462*, 109.

(29) Niyogi, S.; Boukhalfa, S.; Chikkannanavar, S. B.; McDonald, T. J.; Heben, M. J.; Doorn, S. K. *J. Am. Chem. Soc.* **2007**, *129*, 1898.

(30) Lefebvre, J.; Finnie, P. *J. Phys. Chem. C* **2009**, *113*, 7536.

(31) Kato, T.; Hatakeyama, R. *J. Am. Chem. Soc.* **2008**, *130*, 8101.

(32) Qian, H.; Georgi, C.; Anderson, N.; Green, A. A.; Hersam, M. C.; Novotny, L.; Hartschuh, A. *Nano Lett.* **2008**, *8*, 1363.

(33) Tan, P. H.; Rozhin, A. G.; Hasan, T.; Hu, P.; Scardaci, V.; Milne, W. I.; Ferrari, A. C. *Phys. Rev. Lett.* **2007**, *99*, 1374021.

(34) Tan, P. H.; Hasan, T.; Bonaccorso, F.; Scardaci, V.; Rozhin, A. G.; Milne, W. I.; Ferrari, A. C. *Physica E* **2008**, *40*, 2352.

(35) Wang, R. K.; Chen, W. C.; Campos, D. K.; Ziegler, K. J. *J. Am. Chem. Soc.* **2008**, *130*, 16330.

(36) Dauber-Osguthorpe, P.; Roberts, V. A.; Osguthorpe, D. J.; Wolff, J.; Genest, M.; Hagler, A. T. *Proteins: Struct., Funct., Genet.* **1988**, *4*, 31–47.

(37) Lebedkin, S.; Hennrich, F.; Kiowski, O.; Kappes, M. M. *Phys. Rev. B* **2008**, *77*, 165429.

(38) Plentz, F.; Ribeiro, H. B.; Jorio, A.; Strano, M. S.; Pimenta, M. A. *Phys. Rev. Lett.* **2005**, *95*, 247401.

(39) Chou, S. G.; Plentz, F.; Jiang, J.; Saito, R.; Nezich, D.; Ribeiro, H. B.; Jorio, A.; Pimenta, M. A.; Samsonidze, G. G.; Santos, A. P.; Zheng, M.; Onoa, G. B.; Semke, E. D.; Dresselhaus, G.; Dresselhaus, M. S. *Phys. Rev. Lett.* **2005**, *94*, 127402.

(40) Blackburn, J. L.; McDonald, T. J.; Metzger, W. K.; Engtrakul, C.; Rumbles, G.; Heben, M. J. *Nano Lett.* **2008**, *8*, 1047.

JP9076883